View metadata, citation and similar papers at core.ac.uk

brought to you by CORE

provided by Elsevier - Publisher Connector

Available online at www.sciencedirect.com

ScienceDirect

Procedia Engineering 81 (2014) 616 – 621

Procedia Engineering

www.elsevier.com/locate/procedia

11th International Conference on Technology of Plasticity, ICTP 2014, 19-24 October 2014, Nagoya Congress Center, Nagoya, Japan

Extrusion behavior and thermoelectric properties of $Bi_2Te_{2.85}Se_{0.15}$ thermoelectric materials

Zhi-Lei Wang, Kenji Matsuoka, Takehiro Araki, Takahiro Akao, Tetsuhiko Onda, Zhong-Chun Chen*

Department of Mechanical and Aerospace Engineering, Graduate School of Engineering, Tottori University, Koyama-minami 4-101, Tottori 680-8552, Japan

Abstract

Highly dense *n*-type $Bi_2Te_{2.85}Se_{0.15}$ bulk thermoelectric materials were fabricated by mechanical alloying (MA) and hot-extrusion techniques. The extrusion behavior, microstructure, texture, thermoelectric and mechanical properties have been investigated. The extruded samples exhibited fine-grained microstructure and preferred grain orientation. The basal planes in the extrudates were preferentially oriented parallel to the extrusion direction. As the extrusion temperature increased, the electrical resistivity was found to decrease, while the Seebeck coefficient and thermal conductivity increased. A largest dimensionless figure of merit value of 0.6 was achieved at room temperature for the sample extruded at 360 °C. Moreover, the extruded samples showed high hardness values.

© 2014 The Authors. Published by Elsevier Ltd. This is an open access article under the CC BY-NC-ND license (http://creativecommons.org/licenses/by-nc-nd/3.0/).
Selection and peer-review under responsibility of the Department of Materials Science and Engineering, Nagoya University

Keywords: Bismuth telluride; Thermoelectric materials; Mechanical alloying; Hot extrusion

1. Introduction

Bi_2Te_3-based compounds have been widely used in various electronic cooling devices such as infrared detectors, microprocessor chips and thermoelectric cooler for laser diodes [1], owing to their excellent thermoelectric performance near room temperature. The conversion efficiency of a thermoelectric device is highly dependent on

* Corresponding author. Tel.: +81-857-31-5707; fax: +81-857-31-5707.
E-mail address: chen@mech.tottori-u.ac.jp

1877-7058 © 2014 The Authors. Published by Elsevier Ltd. This is an open access article under the CC BY-NC-ND license (http://creativecommons.org/licenses/by-nc-nd/3.0/).
Selection and peer-review under responsibility of the Department of Materials Science and Engineering, Nagoya University
doi:10.1016/j.proeng.2014.10.049

dimensionless thermoelectric figure of merit (*ZT*) of the materials ($ZT=\alpha^2T/(\rho\kappa)$, where α, ρ, κ, and T are the Seebeck coefficient, electrical resistivity, thermal conductivity, and absolute temperature, respectively). Low conversion efficiency limits the practical applications of the thermoelectric materials. Currently, a lot of work has been done on the fabrication of Bi_2Te_3-based alloys to improve the thermoelectric performance, such as unidirectional solidification (zone melting [2] or the Bridgman method [3]) and powder metallurgy (typically, hot-pressing [4]) techniques. The unidirectionally solidified materials present a high figure of merit *ZT* at room temperature, but their mechanical strength is very poor due to large grain sizes and existence of cleavage planes. On the other hand, although hot-pressed materials exhibit high mechanical strength, unfortunately, the thermoelectric performance is not satisfied.

Bi_2Te_3 compound has a rhombohedral structure, which is easy to cleave along the basal plane due to existence of the Te–Te layer parallel to the basal plane, connected by the van der Waals bond [5]. The thermoelectric properties are better in the directions parallel to the basal plane than to the c-axis [6]. Mechanical alloying (MA) and hot-extrusion techniques are considered to be an effective way to fabricate Bi_2Te_3-based compounds with oriented fine grains, so as to improve both the thermoelectric and mechanical properties. Recently, our group has fabricated *p*-type Bi_2Te_3-based bulk materials by MA and hot-extrusion techniques [7], and the results indicated that the extruded materials have excellent thermoelectric and mechanical performance.

In the present work, the MA and hot-extrusion techniques were applied to preparation of *n*-type Bi_2Te_3-based bulk thermoelectric materials. The purpose was to clarify the effect of some extrusion conditions on extrusion behavior, microstructure, texture, thermoelectric and mechanical properties.

2. Experimental Procedure

High purity Bi, Te, and Se powders (>99.9% purity) were used as the starting materials. The powders with a nominal composition of $Bi_2Te_{2.85}Se_{0.15}$ were mechanically alloyed under 200 rpm for 12 h in a purified argon atmosphere using a planetary ball milling system, to refine the powder sizes and promote the reactions between the raw powders. Subsequently, the well reacted powder mixture was pressed into a cylindrical green compact (30 mm in diameter and 25 mm in height) by uniaxial pressing, and used as an extrusion billet. Hot extrusion was performed in a temperature range of 340-450 °C with an extrusion ratio of 25:1 at a punch speed of 1 mm/min.

The density of the extruded samples was determined by the Archimedes method. Phase identification was analyzed by X-ray diffraction (XRD). Orientation imaging microscopy (OIM) analysis was performed using a scanning electron microscope (SEM) equipped with an electron backscattered diffraction (EBSD) system.

The Seebeck coefficient and electrical resistivity of the samples were simultaneously measured using a thermoelectric property test apparatus (ULVAC-RIKO, ZEM-3). The thermal conductivity was measured by laser flash method (NETZSCH, LFA457 Micro Flash). In the thermal conductivity measurements, the direction of the heat flux was set to the extrusion direction. The dimensionless figure of merit of the samples was calculated by the equation of $ZT=\alpha^2T/(\rho\kappa)$. Moreover, the mechanical properties at room temperature were evaluated by the Vickers hardness tests at a load of 1.96 N.

3. Results and Discussion

3.1 Synthesis of $Bi_2Te_{2.85}Se_{0.15}$ compound and its extrusion behavior

The XRD patterns of the powders as-mixed and as-MAed for 12 h are shown in Fig. 1. It can be seen from Fig. 1(b) that the peaks attributed to the raw powders disappeared and the broadened peaks from $Bi_2Te_{2.85}Se_{0.15}$ phase grew instead after MA. The powders prepared by MA for 12 h can be regarded as a single-phase $Bi_2Te_{2.85}Se_{0.15}$ solid solution. Therefore, all samples were fabricated by using the powder prepared by MA for 12 h.

Fig. 2 illustrates the extrusion pressure–stroke curves at different temperatures. In the initial period, the billet is compacted in the container, resulting in a gradual increase in pressure. As the billet is further compacted and flows into the die, the pressure abruptly increases. The extrusion begins at the point where the pressure attains a peak or the pressure gradient starts to relax. During the steady extrusion stage, the pressure change was small. As extrusion

temperature decreased, the pressure level increased. This is attributed to the increase in the deformation resistance of the billet at lower temperatures.

Fig. 3 shows the appearances of the samples extruded at different temperatures. It is shown that all the samples exhibited sound appearances and no evident defects were observed. Furthermore, all the extrudates had high relative density values of >98%. These results indicate that dense, crack-free and single phase $Bi_2Te_{2.85}Se_{0.15}$ bulk extrudates can be obtained under the conditions used in the present work.

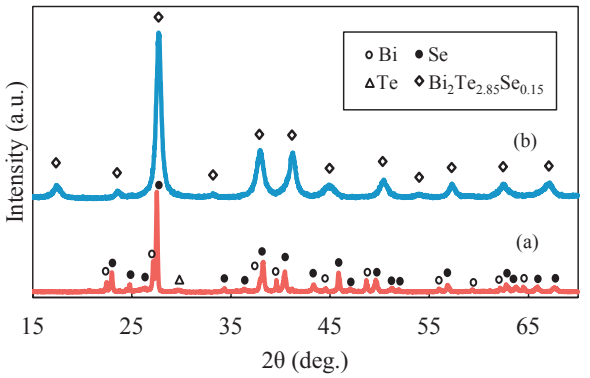

Fig. 1. XRD patterns of (a) as-mixed and (b) as-MAed powders.

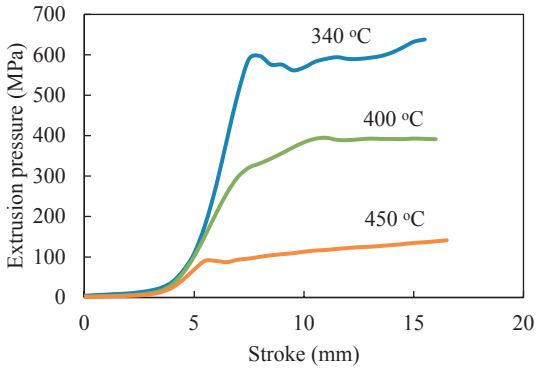

Fig. 2. Extrusion pressure–stroke curves at different temperatures.

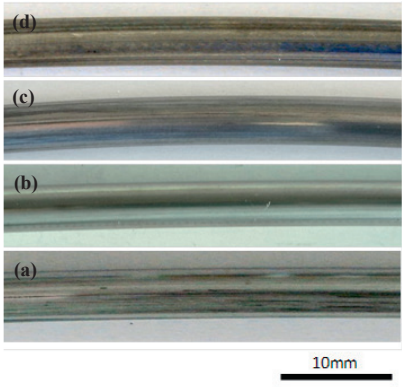

Fig. 3. Appearances of the samples extruded at (a) 340 °C, (b) 360 °C, (c) 400 °C, and (d) 450 °C.

3.2 Microstructure and texture of the extrudates

Fig.4 illustrates the XRD patterns measured on the longitudinal section whose normal direction is perpendicular to the extrusion direction (ED) and transverse section of the sample hot-extruded at 360 °C. As a reference, the pattern of as-MAed powder is also included in Fig. 4. The crystalline orientations are quite different between the longitudinal and transverse sections. The longitudinal section exhibited much stronger diffraction intensities on basal planes such as (0 0 6) and (0 0 15). These results indicate that the basal planes of the grains after the hot extrusion are preferentially oriented parallel to the extrusion direction. Similar results have also been confirmed for the samples extruded at other temperatures.

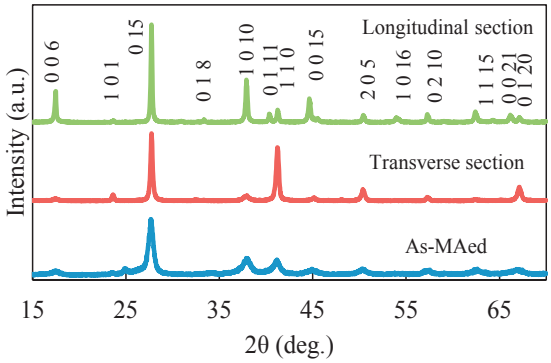

Fig. 4. XRD patterns on the longitudinal and transverse sections of the sample hot-extruded at 360 °C.

The OIM maps on the longitudinal sections of the hot-extruded samples are shown in Fig. 5. The microstructure of the sample extruded at 340 °C is characterized by fine and equiaxed grains. This is likely to be due to the dynamic recrystallization during the hot extrusion and static recrystallization after the extrusion [8]. With the increase in extrusion temperature, the grains grow up gradually. The average grain sizes were measured as 0.55 μm, 0.77 μm, and 1.16 μm at 340 °C, 360 °C, and 400 °C, respectively. Accordingly, with the help of mechanical alloying and hot-extrusion process, fine-grained microstructure with a submicron order can be obtained at extrusion temperatures of <400 °C. From the OIM maps shown in Fig. 5, it can be found that the majority of the grains in the extruded samples are oriented to (0 0 0 1) basal plane. Fig. 6 shows (0 0 0 1) pole figures of the hot-extruded samples, which were obtained from the EBSD analysis. It is clearly shown that the (0 0 0 1) basal plane is predominantly oriented parallel to the extrusion direction. This is in good agreement with those results of the XRD analysis and OIM observations shown in Figs. 4 and 5, respectively.

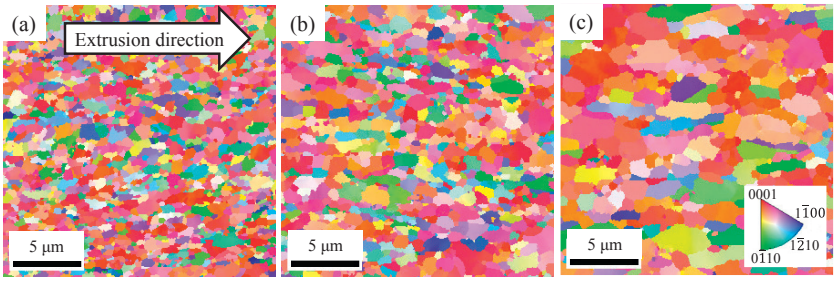

Fig. 5. OIM maps on longitudinal sections of the samples extruded at (a) 340 °C, (b) 360 °C, and (c) 400 °C.

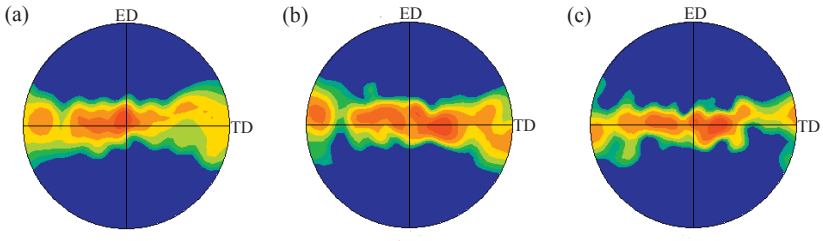

Fig. 6. (0001) pole figures of the samples extruded at (a) 340 °C, (b) 360 °C, and (c) 400 °C.

3.3 Thermoelectric and mechanical properties

Fig. 7 shows the temperature dependence of the Seebeck coefficient. As the extrusion temperature rose, the level of the Seebeck coefficient was reduced. This might be associated with the microstructural changes at different temperatures. Microstructural examinations have found that a Te-rich phase was formed at higher temperatures because Te easily dissociates from $Bi_2Te_{2.85}Se_{0.15}$ matrix due to its high vapor pressure at high temperatures [9]. The formation of Te-rich phase leads to decrease of Te concentration in the matrix, thus resulting in decrease in the Seebeck coefficient.

Fig. 8 shows the temperature dependence of electrical resistivity. A lower extrusion temperature gave rise to larger electrical resistivity. That is because a lower extrusion temperature leads to formation of a fine-grained microstructure, hence resulting in increases in scattering of carriers and thus electrical resistivity. Another reason is related to more residual lattice defects in the samples extruded at a lower extrusion temperature.

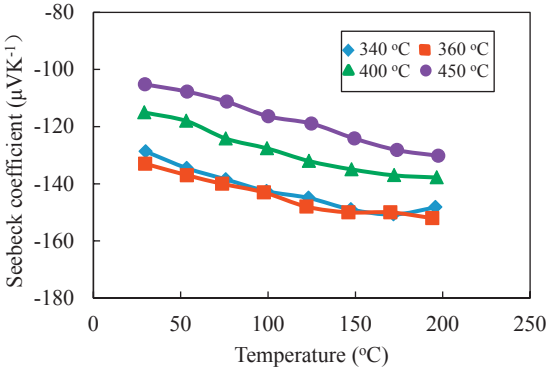

Fig. 7. Temperature dependence of the Seebeck coefficient of the hot-extruded samples.

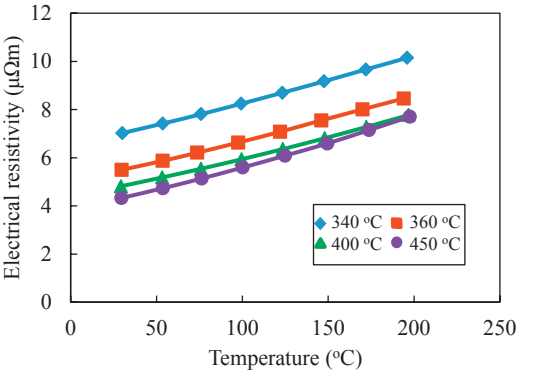

Fig. 8. Temperature dependence of electrical resistivity of the hot-extruded samples.

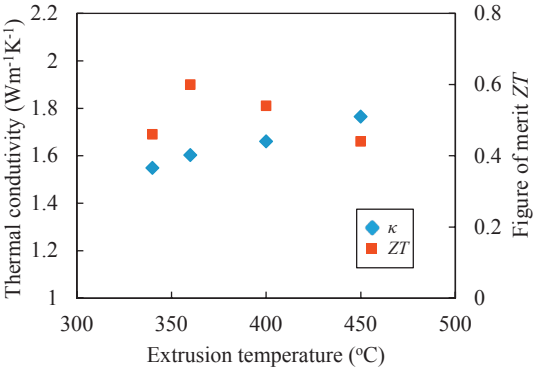

Fig. 9. Extrusion temperature dependence of thermal conductivity and figure of merit (*ZT*) at room temperature.

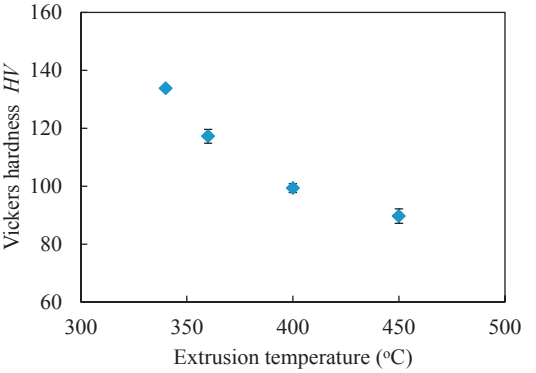

Fig. 10. Extrusion temperature dependence of Vickers hardness.

Fig. 9 shows the extrusion temperature dependence of thermal conductivity and figure of merit (*ZT*). The thermal conductivity slightly increased with increasing the extrusion temperature. Obviously, this results from the

grain growth at higher extrusion temperatures. A large grain size causes decreases in scattering from grain boundaries, hence resulting in increases of thermal conductivity. As a result, a largest *ZT* value of 0.6 was obtained at room temperature for the sample extruded at 360 °C, as shown in Fig. 9.

Fig. 10 shows the Vickers hardness as a function of extrusion temperature. The hardness monotonically decreased with increasing the extrusion temperature. A possible reason for this tendency is that a lower extrusion temperature results in a smaller average grain size. The Vickers hardness of the sample extruded at 340 °C showed 1.5 times higher than the sample extruded at 450 °C.

4. Conclusions

Sound and dense *n*-type $Bi_2Te_{2.85}Se_{0.15}$ bulk thermoelectric materials have been successfully fabricated by mechanical alloying and hot-extrusion techniques. The combination of mechanical alloying and hot extrusion resulted in significant grain refinement and preferential orientation. Fine-grained microstructure with a submicron order were obtained at extrusion temperatures of <400 °C. The basal planes in the extrudates were preferentially oriented parallel to the extrusion direction. As the extrusion temperature increased, the electrical resistivity was found to decrease, whereas the Seebeck coefficient and thermal conductivity increased. A largest dimensionless figure of merit value of 0.6 was achieved at room temperature for the sample extruded at 360 °C. Furthermore, although the Vickers hardness was reduced with increasing the extrusion temperature due to grain growth, the extruded samples exhibited high hardness values.

Acknowledgements

The authors would like to thank Profs. Shigekazu Morito and Hiroyuki Kitagawa of Shimane University for their experimental supports and fruitful discussion. This work was supported in part by Japan Science and Technology Agency and the Amada Foundation.

References

[1] Im, J.T., Hartwig, K.T., Sharp, J., 2004. Microstructural refinement of cast p-type Bi_2Te_3–Sb_2Te_3 by equal channel angular extrusion. Acta Materialia 52, 49-55.

[2] Taylor, P. J., Maddux, J. R., Jesser, W. A., Rosi, F. D., 1999. Room-temperature anisotropic, thermoelectric, and electrical properties of n-type $(Bi_2Te_3)_{90}(Sb_2Te_3)_5(Sb_2Se_3)_5$ and compensated p-type $(Sb_2Te_3)_{72}(Bi_2Te_3)_{25}(Sb_2Se_3)_3$ semiconductor alloys. Journal of Applied Physics 85, 7807-7813.

[3] Yim, W. M., Rosi, F. D., 1972. Compound tellurides and their alloys for peltier cooling − A review. Solid State Electronics 15, 1121.

[4] Yang, J.Y., Aizawa, T., Yamamoto, A., Ohta, T., 2000. Effects of interface layer on thermoelectric properties of a pn junction prepared via the BMA-HP method. Journal of Alloys and Compounds 312, 326-330.

[5] Weise, J.R., Muller, L., 1960. The crystal structure of $Bi_2Te_{3-x}Se_x$. Journal of Physics and Chemistry of Solids 15, 13.

[6] Schulz, L. G., 1949. A method of determining preferential orientation for reflected sheet sample by X-ray instrument. Journal of Applied Physics 20, 1030.

[7] Nagami, Y., Matsuoka, K., Akao, T., Onda, T., Hayashi, T., Chen, Z. C., 2014. Preparation and characterization of $Bi_{0.4}Sb_{1.6}Te_3$ bulk thermoelectric materials. Journal of electronic materials DOI:101007/s11664-014-3038-0.

[8] Chen, Z. C., Suzuki, K., Miura, S., Nishimura, K. Ikeda, K., 2009. Microstructural features and deformation-induced lattice defects in hot-extruded Bi_2Te_3 thermoelectric compound. Materials Science and Engineering: A 500, 70-78.

[9] Yoneda, D., Kato, M., Ohsugi, I. J., 2010. Anomaly in the specific heat of lead tellurides. Journal of Applied Physics 107, 074901.